CVGIP: GRAPHICAL MODELS AND IMAGE PROCESSING
Vol. 56, No. 2, March, pp. 140–148, 1994

Multiresolution Adaptive Image Smoothing

PETER MEER

Department of Electrical and Computer Engineering, Rutgers University, P.O. Box 909, Piscataway, New Jersey 08855-0909

RAE-HONG PARK

Department of Electronic Engineering, Sogang University, P.O. Box 1142, Seoul, 100-611, Korea

AND

KYUJIN CHO

Department of Electrical and Computer Engineering, Rutgers University, P.O. Box 909, Piscataway, New Jersey 08855-0909

Received December 10, 1992; revised November 9, 1993; accepted December 7, 1993

A hierarchical image smoothing method is presented which does not require user specified parameters. For every pixel the largest centered window (7 × 7, 5 × 5 or 3 × 3) containing a constant patch is sought. The selection is made by comparing a locally computed homogeneity measure with its robust global estimate. If the window is declared homogeneous, the pixel is assigned the spatial average. Around discontinuities an adaptive least squares smoothing method is applied for 3 × 3 windows. The performance of the algorithm is compared with several other smoothing techniques for additively corrupted images. The smoothing of synthetic aperture radar images is used as an example for multiplicative noise.

1. INTRODUCTION

In noisy images the effectiveness of feature extraction is reduced since the corrupted data may significantly deviate from the assumed model. To improve performance a noisy image often is smoothed before being processed. An efficient smoothing algorithm must satisfy three conditions.

—Should be a parallel process at the pixel level. The value of the smoothed pixel is then computed in a small window centered on it. Successive iterations of the same procedure will extend the "region of influence" beyond the bounds of the processing window.

—Should not incorporate assumptions about the distribution of the corrupting noise. (On the other hand, the additive or multiplicative nature of the noise should be taken into account.) Since smoothing is based on a small region, the sample statistics may not represent the real distribution and erroneous decisions can be taken. Iterations also modify the characteristics of the noise.

—Should preserve significant discontinuities. This can only be achieved with adaptive smoothing algorithms which exhibit a different behavior, whenever, prior to smoothing, a discontinuity is detected in the processing window.

The facet model based smoothing of Haralick and Watson [6] was among the first smoothing algorithms described in the computer vision literature which satisfied all the above conditions. Given a window size, the same order polynomial surface is fitted to the data in every window to which a pixel belongs. For example, if the window is 3 × 3 there are nine different least squares fits. The smoothed value of the pixel is taken from the window yielding the smallest residual power (variance). This criterion prefers windows with homogeneous regions and thus smoothing tends to preserve the discontinuities in the image. We will apply the algorithm with constant surfaces and refer to it as *constant-facet smoothing*.

The cases of additive and multiplicative noise are distinguished in adaptive smoothing algorithms although most methods can be applied for both types of perturbations. For additive noise excellent reviews can be found in Saint-Marc *et al.* [22] for the computer vision literature, and in McLean and Jernigan [14] for the image processing literature. Adaptive smoothing methods assume piecewise constant image structure. Saint-Marc *et al.* [22] compute the modulus of the gradient vector at every pixel and use it to generate the Gaussian weights of a smoothing filter in a 3 × 3 window. The variance of the Gaussian is a free parameter of the method. The larger the gradient (the more probable the presence of a discontinuity), the less the pixel contributes to the smoothed value at the center of the window. The similar anisotropic diffusion

1049-9652/94 $6.00

algorithm of Perona and Malik [18] implements the discrete diffusion equation with barriers defined from adjacent pixel differences. These barriers stop the diffusion (i.e., smoothing) at image discontinuities. Recently, Crespo and Schafer [3] proposed incorporation of a morphological edge detection procedure at each iteration of the algorithm. We will refer to the algorithm of Saint-Marc *et al.* [22] as *diffusion smoothing*. Both the constant-facet and diffusion smoothing are iterative methods with no clearly defined stopping criterion.

In applications the most frequently met multiplicative noise case is that of speckle noise. Speckle in images is due to the interference patterns which appear when coherent illumination is scattered at surfaces having irregular shapes at the scale of the wavelength used. See, for example, Goodman [5] for a description of the physical phenomena involved in generation of speckle. Speckle appears in images as a superposed fine granular texture having signal-dependent values. The removal of speckle is a very important problem and is encountered in coherent images such as synthetic aperture radar (SAR) images, laser images, and ultrasonic images.

When logarithmically transformed, the speckle noise becomes additive and signal-independent [1] and various homomorphic filters have been considered for smoothing [11]. To process SAR data Frost *et al.* [4] adapted a least mean square error filter according to the local mean and standard deviation. Morphological techniques have also been employed for speckle suppression. Crimmins [2] proposed an iterative nonlinear algorithm using the umbra concept, Safa and Flouzat [21] alternatively suppressed the local minima and maxima in the noisy image with closing and opening operations. Adaptive smoothing can also be achieved employing other minimization criterion. Mahesh *et al.* [13] used the minimum-error minimum-correlation criterion. Lopes *et al.* [12] compares the performance of several filters for SAR images.

Two problems are to be faced by any adaptive smoothing technique. A reliable measure for the presence of a discontinuity in the processing window must be available. The structure of the filter then depends on this measure to avoid smoothing over an edge. Methods which employ user supplied parameters as decision thresholds have their performance strongly dependent on how close the user was able to guess the optimal value. The main novelty of our algorithm is that *all* the parameters controlling the adaptive behavior are robustly derived from the input image.

The second problem of an adaptive algorithm is related to the size of the processing window. The larger a window the better the achieved smoothing. However, in a larger window the probability of a significant discontinuity being present also increases, while the chances of detecting such a discontinuity may decrease. We avoid this problem through a hierarchical approach. The value of a smoothed pixel is computed from one of a few windows of increasing sizes centered on that pixel. The selection of the window best representing the smoothed pixel is automatically performed by the algorithm after a robust analysis.

The paper is organized as follows. In Section 2 the adaptive least squares filtering is succinctly reviewed. The proposed multiresolution adaptive least squares smoothing (MAS) algorithm is described in Section 3. Application of the algorithm to images corrupted with additive noise and comparison of the results with those obtained by other techniques is in Section 4. The case of multiplicative noise is treated in Section 5. In Section 6 the paradigm behind the proposed algorithm is discussed.

2. ADAPTIVE LEAST SQUARES SMOOTHING

Similar to most smoothing algorithms it is assumed that the image has a piecewise constant structure. This model yields the maximum possible smoothing, and since the algorithm is applied at every pixel the amount of introduced artifacts is usually not severe. The adaptive least squares smoothing filter first proposed by Lee [9] will be employed for the task of preserving the local image structure around the step discontinuities. Kuan *et al.* [7] and Unser [24] gave similar formulations for these filters.

Let $f(i, j)$ be the value of the pixel at site (i, j) in the uncorrupted (original) image. The noisy image $g(i, j)$ is then additively corrupted

$$g(i, j) = f(i, j) + n(i, j) \tag{1}$$

with $n(i, j)$, a signal-dependent, zero-mean, white noise process having the nonstationary variance $\sigma_n^2(i, j)$. Since only one instance of the random processes is available for the pixel (i, j) we must assume local ergodicity in the first and second-order statistics. That is, when characterizing the distributions from which $f(i, j)$ and $n(i, j)$ were obtained, the ensemble statistics are considered equal with the spatial counterparts computed in a small $(2p + 1) \times (2p + 1)$ window centered on the pixel (i, j).

The least squares estimator of the uncorrupted pixel value $\hat{f}(i, j)$ given the noisy data $g(i, j)$ is (see Lee [9] or Kuan *et al.* [7] for details)

$$\hat{f}(i, j) = [1 - k(i, j)]\, \bar{g}(i, j) + k(i, j)\, g(i, j). \tag{2}$$

The weights $k(i, j)$ are

$$k(i, j) = \frac{s_f^2(i, j)}{s_f^2(i, j) + \sigma_n^2(i, j)}, \tag{3}$$

where $\bar{g}(i, j)$ is the spatial average computed in the window from the noisy image; $s_f^2(i, j)$, the spatial variance of the original image in the same window. The latter will be defined function of known quantities. The estimator

(2) does not have a linear structure since the weight $k(i, j)$ does depend on the data in the neighborhood of the estimated pixel. If the spatial variance of the original image in the window, $s_f^2(i, j)$, is small relative to the noise variance $\sigma_n^2(i, j)$, the weight is close to zero and the estimate reproduces the spatial average of the window; i.e., a strong smoothing is achieved. Such situation appears when the region in the window is almost constant and/or the signal-to-noise ratio $s_f^2(i, j)/\sigma_n^2(i, j)$ very low. In both cases smoothing is desirable. If $s_f^2(i, j)$ dominates $\sigma_n^2(i, j)$ a discontinuity is assumed to be present in the window. It is important to emphasize that the assumption is correct only for step discontinuities [15]. The weight is now close to one and the estimate reproduces the available data, i.e., less smoothing is introduced. Thus, the adaptive behavior of the algorithm is tuned toward preserving step discontinuities. The adaptive least squares algorithm is not robust in statistical sense since the computation of the parameters (variances) is not immune to outliers.

The spatial variance of the original data $s_f^2(i, j)$ can be determined once the nature of the noise is specified. The first case is that of stationary, additive, signal-independent noise, with variance σ_n^2, the usual assumption in computer vision applications. It is immediate to obtain from (1)

$$s_f^2(i, j) = s_g^2(i, j) - \sigma_n^2, \tag{4}$$

where $s_g^2(i, j)$ is the spatial variance computed in the $(2p + 1) \times (2p + 1)$ window centered on the pixel in the noisy image.

The other important case is that of multiplicative noise. Instead of the model (1) the following noise model is assumed [7]:

$$g(i, j) = f(i, j)\, u(i, j), \tag{5}$$

where $u(i, j)$ is a noise process independent of $f(i, j)$. The multiplicative noise $u(i, j)$ has mean $E[u(i, j)] = 1$ and stationary variance σ_u^2. The expression (5) can also be written as

$$g(i, j) = f(i, j) + [u(i, j) - 1]\, f(i, j) \tag{6}$$

and comparing (6) with (1) a signal-dependent additive noise component can be defined

$$n(i, j) = [u(i, j) - 1]\, f(i, j). \tag{7}$$

Thus the multiplicative noise case is reduced to the additive, zero-mean, signal-dependent noise case. The variance of this noise process can now be computed as

$$\sigma_n^2(i, j) = E[n^2(i, j)] = \sigma_u^2[[\bar{g}(i, j)]^2 + s_f^2(i, j)] \tag{8}$$

where the ergodicity assumption was again employed. Since the noise $u(i, j)$ and the original data $f(i, j)$ are independent, the variance of the noisy pixel is

$$\begin{aligned} s_g^2(i, j) &= s_f^2(i, j) + \sigma_n^2(i, j) \\ &= s_f^2(i, j) + \sigma_u^2[[\bar{g}(i, j)]^2 + s_f^2(i, j)] \end{aligned} \tag{9}$$

from where

$$s_f^2(i, j) = \frac{s_g^2(i, j) - \sigma_u^2[\bar{g}\,(i, j)]^2}{1 + \sigma_u^2} \tag{10}$$

To conclude this section, we remark that the parameters characterizing the noise, σ_n^2 in the additive case, and σ_u^2 in the multiplicative case, must be known in order to be able to use the estimator (2). In the next section we combine a robust method for estimating these parameters with a decision process for the selection of an optimal p, i.e., optimal window size for every pixel.

3. MULTIRESOLUTION ADAPTIVE SMOOTHING

In our multiresolution approach a pixel is considered to be the center of several windows of decreasing sizes. Let p be the size parameter of the $(2p + 1) \times (2p + 1)$ window and $p_{\max}$ its maximum value. The ideal case is when the window contains a homogeneous (constant in the original image) patch. Smoothing is achieved by the center pixel being replaced with the spatial average computed in that window. The larger the window, the more smoothing is introduced and thus the proper choice of $p_{\max}$ allows smoothing of a homogeneous region without employing iterative procedures. The value of $p_{\max}$ is limited upward by the requirement of local computation and by the loss of sensitivity to image structure. We chose $p_{\max} \leq 3$ corresponding to a 7×7 maximum window size. Thus at every pixel the following centered windows can be defined: 7×7, 5×5, and 3×3. We will refer to these windows as different resolutions at which the image is analyzed.

A useful smoothing algorithm must preserve the significant discontinuities (step-edges, by the assumed image structure) of the image. The adaptive least squares procedure described in Section 2 can be employed for this task. When larger windows are used, a fine detail in the image may not increase $s_f^2(i, j)$ sufficiently to produce a significant change in the weight $k(i, j)$. Thus, when adaptive behavior is called for, the smallest 3×3 window should be used. Since the adaptive least squares algorithm tends to retain the available data if a discontinuity is detected, the use of a small window does not degrade the overall performance.

Computation of the weights (3) require a reliable estimate for the noise variance. To obtain this estimate the following assumption about the *global* structure of the image should be made.

Homogeneity conjecture. At the lowest resolution ($p = p_{max}$) the number of windows containing a homogeneous patch in the noisy image should be close to or exceed the number of windows located over discontinuities.

If the conjecture is strongly violated, the image is dominated by texture and smoothing is not appropriate. Otherwise the algorithm will perform satisfactorily as the analysis of the experimental results will show. The validity of the conjecture for smaller windows (higher resolutions) is implicit. Assumptions about the structure of the image are central for an adaptive smoothing algorithm, but they usually relate to local and not to global characteristics. Lopes *et al.* [12] use the term "scene heterogeneity" in this context, McLean and Jernigan [14] compare 14 different, mostly local, image structure measures.

In every window centered on the pixel (i, j), a scalar homogeneity measure $\gamma^2(i, j)$, will be defined. If no discontinuity is contained in the window, $\gamma^2(i, j)$ should depend only on the characteristics of the noise corrupting the image. The presence of a significant discontinuity should increase its value. For the piecewise constant image structure model, spatial variances are reliable homogeneity measures [15]. A constant patch in the original image has $s_f^2(i, j) = 0$ and thus (4) for additive noise $\gamma^2(i, j) \triangleq s_g^2(i, j)$. In homogeneous windows under stationary additive noise the spatial variance computed in the noisy image is an unbiased estimate of σ_n^2. Similarly, from (10) we can define for multiplicative noise

$$\gamma^2(i, j) \triangleq \frac{s_g^2(i, j)}{[\bar{g}(i, j)]^2} \tag{11}$$

which for homogeneous regions is an unbiased estimate of σ_u^2.

It is not known a priori which window is homogeneous. The obtained $\gamma^2(i, j)$ values are ordered in a sequence which represents the distribution of the homogeneity measure for the given image and the employed resolution of $(2p + 1) \times (2p + 1)$ windows. From the homogeneity conjecture we can conclude that the distribution must have a strong mode. Indeed, about half of the values in the sequence must be distributed around Γ^2, the expected value for homogeneous windows. Most of the remaining $\gamma^2(i, j)$ values are spread along the upper tail of the sequence. A simple mode detection procedure can estimate Γ^2. The mode estimator is a robust estimator, tolerating up to half of the data being outliers, i.e., not belonging to the distribution of the majority [20, Chap. 4]. The mode of a random variable corresponds to the maximum of its probability density function. Therefore in the ordered sequence many samples should cluster around the mode which is detected from the interval with the most samples in the sequence. The mode detection algorithm is available in packages (e.g., [19, p. 462]).

The mode Γ^2 provides the robust global estimate for the stationary noise variance σ_n^2 or σ_u^2. Being based on the largest possible number of local variance estimates, Γ^2 must be close to the true value of the variance. At every resolution $p = 1, 2, 3$ a separate distribution of $\gamma_p^2(i, j)$ is obtained. The global estimates Γ_p^2 can then be used to choose the optimal window size from which the smoothed pixel value is determined. Whenever the homogeneity measure computed in a window is less or equal to the stationary noise variance estimate; i.e., $\gamma_p^2(i, j) \leq \Gamma_p^2$, the window should contain in the original image a constant patch with a very high probability.

At every pixel and every resolution the binary variables $c_p(i, j)$ can now be defined:

$$c_p(i, j) = \begin{cases} 1 & \text{if } \gamma_p^2(i, j) \leq \Gamma_p^2 \\ 0 & \text{if } \gamma_p^2(i, j) > \Gamma_p^2 \end{cases}. \tag{12}$$

Note that the values of $c_p(i, j)$ can be computed independently. The optimal resolution for a pixel is selected as the largest $p \leq p_{max}$ for which $c_p(i, j) = 1$, and the pixel is substituted with the spatial average computed in that window. Pixels not having any $c_p(i, j) = 1$ are assumed to be adjacent to a step discontinuity and the smoothed value is estimated in the 3×3 window with the adaptive least squares procedure. The proposed multiresolution adaptive smoothing (MAS) algorithm can be summarized as follows:

For $p = 1, \ldots, p_{max} \leq 3$:

1. At every pixel compute in a $(2p + 1) \times (2p + 1)$ window:
   - —the spatial average of the noisy image $\bar{g}_p(i, j)$;
   - —the spatial variance of the noisy image $s_{g,p}^2(i, j)$;
   - —the homogeneity measure $\gamma_p^2(i, j)$.
2. Estimate the mode of the homogeneity measure sequence Γ_p^2.
3. Compute the values $c_p(i, j)$.

The value of the pixel in the smoothed image is

$$\hat{f}(i, j) = \begin{cases} \bar{g}_p(i, j) & \text{if } p = \max_p [c_p(i, j) = 1] \geq 1 \\ [1 - k(i, j)] \quad \bar{g}_1(i, j) + k(i, j)\, g(i, j) & \\ \qquad \text{if } c_p(i, j) = 0 \text{ for } p = 1, \ldots, p_{max}. & \end{cases}$$

4. EXPERIMENTAL RESULTS: ADDITIVE NOISE CASE

The mode of the $\gamma_p^2(i, j)$ sequence is the robust global estimate of the stationary noise variance, $\hat{\sigma}_{n,p}^2$, based on $(2p + 1) \times (2p + 1)$ windows. The weight $k(i, j)$ used in

the adaptive smoothing procedure becomes, after combining (3) and (4),

$$k(i,j) = \frac{\gamma_1^2(i,j) - \Gamma_1^2}{\gamma_1^2(i,j)}. \quad (13)$$

Note that $\gamma_1^2(i, j)$ must be larger than Γ_1^2 in order the adaptive smoothing to be employed.

The performance of the multiresolution adaptive smoothing algorithm was compared with the constant-facet smoothing [6] and the diffusion smoothing methods [22] discussed in Section 1. These methods require parameters provided by the user. In both constant-facet and diffusion smoothing the number of iterations must be specified if oversmoothing is to be avoided. The quality of diffusion smoothing also depends on the value of the diffusion constant. When comparing the different techniques, all the parameters were tuned to obtain visually optimal outputs. No parameters are required for the MAS algorithm.

In Fig. 1a the *house* image is shown. One iteration of constant-facet smoothing (Fig. 1b) and diffusion smoothing (Fig. 1c) were applied with 3 × 3 windows. These methods achieve satisfactory smoothing of large homogeneous regions. However, also introduce artifacts in the more textured parts of the image were the employed criterion for discontinuity detection fails and oversmoothing results. See for example the tree at the right. When only 3 × 3 windows are used for the MAS algorithm (Fig. 1d) 22.4% of the windows were declared homogeneous and the central pixel substituted with the spatial average. For

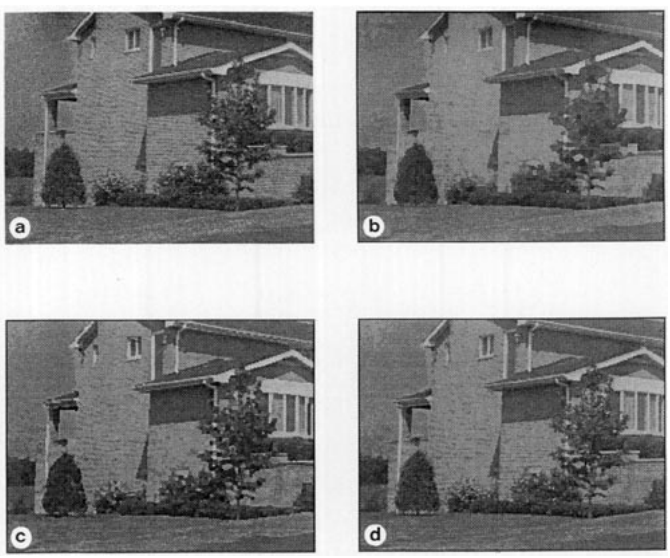

FIG. 1. Different 3 × 3 window based smoothing methods applied to the *house* image. (a) Input image. (b) Constant-facet smoothing, one iteration. (c) Diffusion smoothing, one iteration. (d) Multiresolution adaptive smoothing.

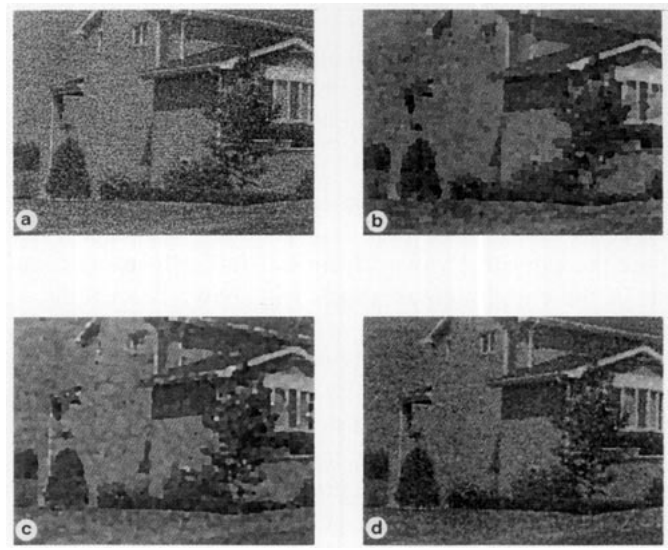

FIG. 2. Different 3 × 3 window based smoothing methods applied to the noisy *house* image. (a) Input image, additive Gaussian noise $\sigma_n^2 = 900$. (b) Constant-facet smoothing, three iterations. (c) Diffusion smoothing, four iterations. (d) Multiresolution adaptive smoothing.

the other pixels the adaptive least squares procedure was used. The image passed practically unchanged.

The difference in performance is emphasized when the image is noisy, corrupted with additive Gaussian white noise having $\sigma_n^2 = 900$ (Fig. 2a). In Fig. 2b the result of the constant-facet smoothing algorithm after three iterations, in Fig. 2c the result of the diffusion smoothing method after four iterations are given. Both methods used 3 × 3 windows and further iterations did not yield significant changes. The presence of small "tiles" in the image is due to local correlations introduced by the iterations. The image smoothed with the MAS algorithm for $p_{\max} = 1$ is shown in Fig. 2d. Again less artifacts are introduced and the fine details are better preserved. Pure smoothing accounted for 40.2% of the pixels, the adaptive least squares procedure for 59.8%. Since the estimated noise variance is used as decision threshold, the percentage of windows declared homogeneous increased relative to the noiseless case. The increase is due to windows containing small step-edges which now are buried in the noise.

The noisy *house* image was also employed for comparison of the MAS algorithm's performance with Lee's [10] adaptive smoothing technique. Lee's method uses a 7 × 7 window. From the window a directional subset of pixels is chosen after local edge detection and the adaptive least squares procedure is applied to these pixels. The user can supply a threshold on the local variance estimate to select only the windows containing significant edges. Lee proposed to improve the local noise variance estimate, used in the computation of the weights, by averaging the five smallest variances associated with the pixels in the 7 × 7 window.

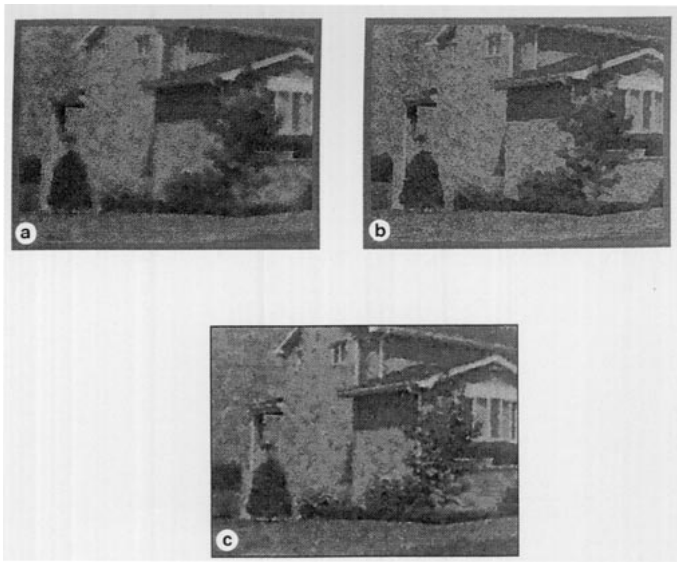

FIG. 3. Smoothing of image in Fig. 2a. (a) Lee's method, without directional subsets. (b) Lee's method, with directional subsets. (c) Multiresolution adaptive smoothing, $p_{max} = 3$.

In Fig. 3a the result of Lee's method is shown, without applying the directional subsets based procedure. The technique thus becomes a one-step adaptive least squares filtering algorithm in 7×7 windows. The local variance estimates often are biased upward by the discontinuities and the image is oversmoothed. In Fig. 3b, directional subsets were used for every pixel. The sharpness of the edges in the smoothed image is improved, however, the quality of homogeneous regions somewhat deteriorates. For comparison, the MAS algorithm was run with $p_{max} = 3$. The result, in Fig. 3c, shows that the hierarchical approach combined with global noise variance estimates, succeeds to find the optimal trade-off between smoothing of homogeneous regions and preserving discontinuities. The three homogeneity measure sequences based on which the smoothed pixel values were established, are shown in Fig. 4 as histograms. The locations of the modes are marked by arrows. The detected values are $\Gamma_3^2 = 976$ for the 7×7 windows, $\Gamma_2^2 = 1106$ for the 5×5 windows, and $\Gamma_1^2 = 1045$ for the 3×3 windows; all close to the true variance of the noise, $\sigma_n^2 = 900$. (The error is around ten percent in the standard deviation values.) The slight systematic increase in the estimated values is due to windows containing small step edges or ramp edges. This increase did not degrade the performance of the algorithm. When the correct variance value was supplied to the algorithm the output did not change significantly. Using the modes as decision threshold, 35.5% of the smoothed values were taken from 7×7 windows, 22.1% from 5×5 windows, 19.7% from 3×3 windows, and the values of the remaining 22.7% of pixels were estimated with the adaptive least squares procedure. Thus the MAS algorithm allocated the pixels evenly across the resolutions in accordance with the image structure.

The MAS and Lee algorithms take different approaches in adapting the shape of the processing window to the local image structure. Near an edge the MAS algorithm will decrease the size of the window while Lee's technique will choose the best suited directional subset. To compare the two approaches, both methods were used as preprocessors for edge detection in a noisy synthetic image (Fig. 5b). The original image (Fig. 5a) contains step edges of all orientations. The image was smoothed (Figs. 5c and 5d) and the edges detected with Canny's edge detector having the two thresholds set to optimal values. Both smoothing methods yield edges of same quality (Figs. 5e and 5f). For data reproducing the assumptions embedded in the algorithms (piecewise constant image structure) the two approaches yield similar performance.

5. EXPERIMENTAL RESULTS: MULTIPLICATIVE NOISE CASE

The mode of the homogeneity measure, $\gamma_p^2(i, j)$, sequence is the estimate of the stationary multiplicative noise variance computed from $(2p + 1) \times (2p + 1)$ homogeneous windows. The weight $k(i, j)$ can be defined for the multiplicative case by combining (3) and (10)

$$k(i,j) = \frac{\gamma_1^2(i,j) - \Gamma_1^2}{\gamma_1^2(i,j)(1 + \Gamma_1^2)}. \tag{14}$$

The value of $\gamma_1^2(i, j)$ must exceed Γ_1^2 in order to use the adaptive filtering procedure.

The multiplicative noise of interest for us is the speckle noise, as was discussed in Section 1. An often used preprocessing step for speckle removal is the average of several images taken independently in different bands. The number of averaged images N is called the number of looks of the final image. The accepted model of speckled images is the gamma distribution. In a homogeneous neighborhood the expected value of a pixel $g(i, j)$ in a N looks speckled image is the uncorrupted pixel value $f(i, j)$, while its variance is $f(i, j)^2/N$. The original pixel value thus can be estimated with $\bar{g}(i, j)$, the spatial average. Since the mean and the variance are proportional, the speckle noise is signal-dependent and can be modeled as multiplicative noise [9, 11]. We must, however, assume that the speckle image is undersampled such that the pixels are independent [23]. Note that, for uncorrupted data the homogeneity measure (11) should be equal to $1/N$.

The performance of the MAS algorithm for SAR images was compared with the method of Kuan *et al.* [8], i.e., the multiresolution approach vs. a one-step procedure. The method of Kuan *et al.* [8] is similar to that of Lee (1981) but does not use the linear approximation of the latter. The *aerial* image (Fig. 6a) was corrupted with

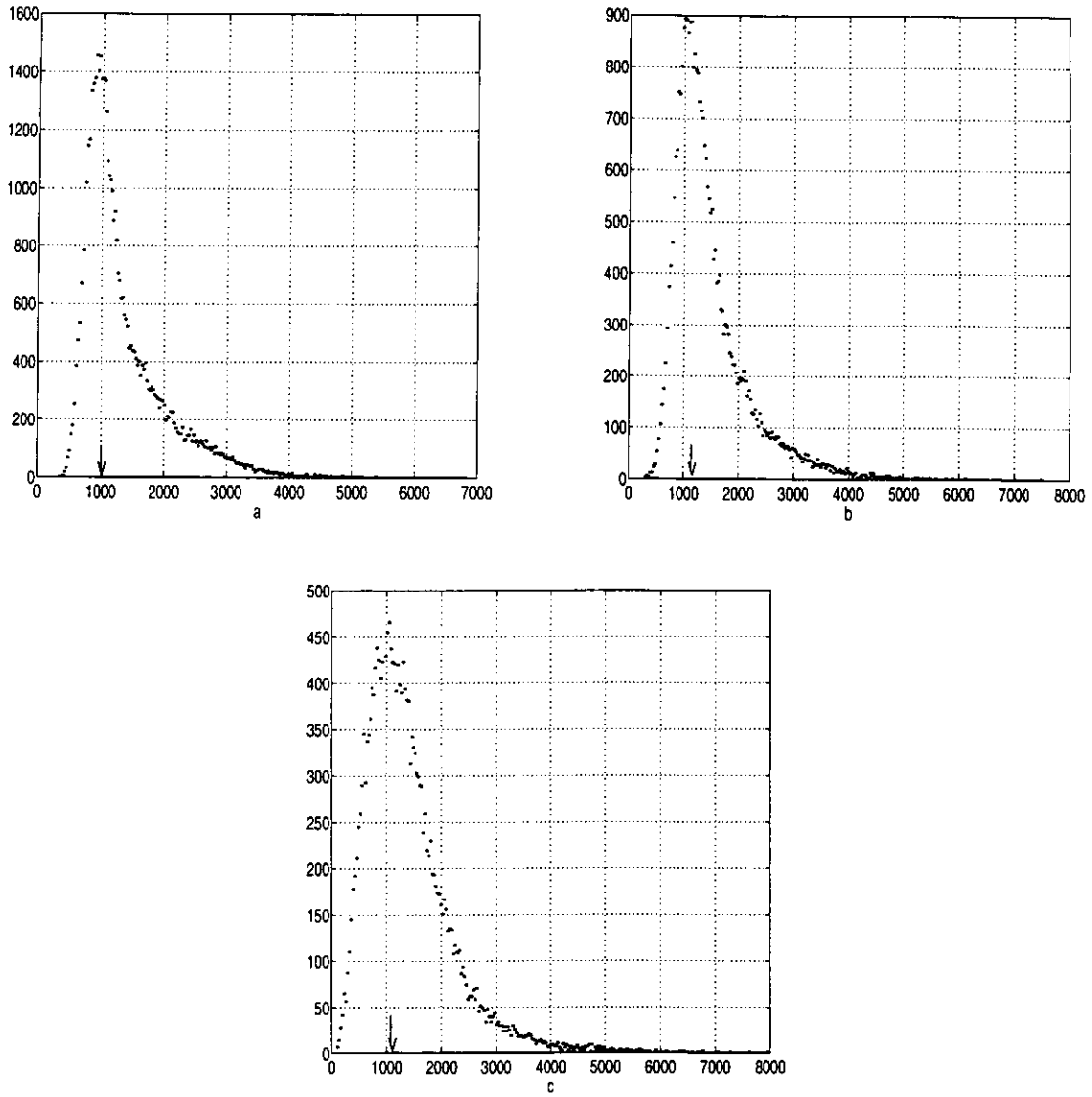

FIG. 4. Distribution of the homogeneity measures extracted from Fig. 3c. (a) 7 × 7 windows (b) 5 × 5 windows (c) 3 × 3 windows. The arrow marks the detected mode.

gamma noise corresponding to four looks (Fig. 6b). The output of the adaptive least squares smoothing algorithm of Kuan *et al.* for 7 × 7 window size is shown in Figure 6c. It is important to emphasize that the multiplicative noise variance $\sigma_u^2 = 0.25$ must be known a priori for this algorithm. The large size of the employed window does not allow smoothing to be performed in a few pixel wide band along the edges. Once a window contains a significant edge, the adaptive algorithm prefers the original data.

The MAS algorithm estimates the values of $\hat{\sigma}_u^2$ from the homogeneity measure sequences and thus it is not required to be supplied by the user. The estimated mode values were $\Gamma_3^2 = 0.29$, $\Gamma_2^2 = 0.34$, and $\Gamma_1^2 = 0.32$. The unsmoothed bands along edges are now significantly reduced since in such regions the MAS algorithm prefers smaller neighborhoods. About 39.5% of the pixels were replaced with the spatial averages computed in 7 × 7 windows, 20.4% in 5 × 5 windows, 16.0% in 3 × 3 windows, and 24.1% by the adaptive least squares estimate. The distribution of the pixels selected at different resolutions is shown in Fig. 7.

To investigate the performance of the MAS algorithm for more realistic SAR images a 128 × 128 image was generated using the SARSIM radar simulator program of The Analytic Sciences Corp. The image is shown in Fig. 8a and the output of the algorithm in Fig. 8b. Note the preservation of all the features in spite of significant smoothing of the background.

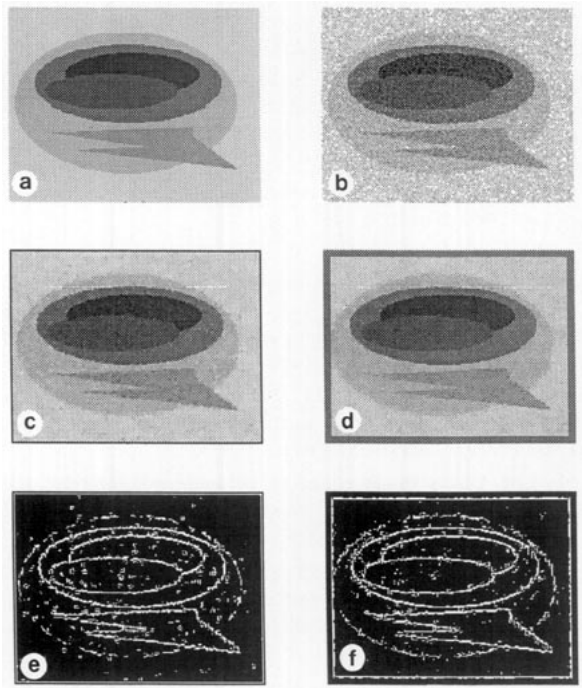

FIG. 5. Preprocessor for edge detection. (a) Original image. (b) Corrupted with additive Gaussian noise, $\sigma^2 = 400$. (c) Smoothed with MAS algorithm. (d) Smoothed with Lee's algorithm. (e) Edge extracted from (c). (f) Edge extracted from (d).

6. DISCUSSION

The principal novelty of the proposed smoothing method is that does not have any free parameter to be set by the user. The noise variance is robustly estimated from the image at several resolutions and used to find the optimal window size for every pixel. Techniques which explicitly detect discontinuities before smoothing in order to choose the best shape for the processing window [10, 25] can be incorporated in the proposed algorithm.

McLean and Jernigan [14] concluded in a study of local image homogeneity measures that most adaptive filtering techniques will perform similarly given that the measures have the same quality. Our robust global estimates for the noise variance are the most reliable ones which can be extracted from a given image. Recently Olsen [16] compared several methods for image noise estimation and found that simple averaging of local estimates from homogeneous windows performed the best. The homogeneous windows were selected after local edge detection. Our

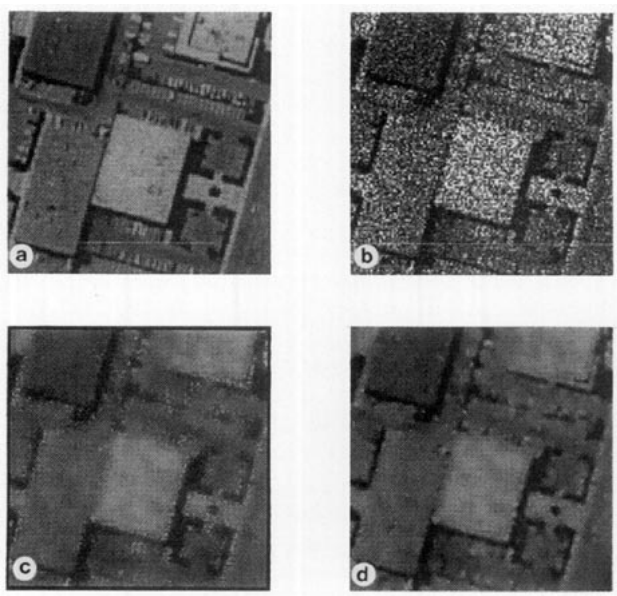

FIG. 6. Smoothing of SAR images. (a) Original image. (b) The simulated four-looks SAR image. (c) Smoothing with the Kuan *et al.* [8] algorithm in a 7 × 7 window. (d) Multiresolution adaptive smoothing with $p_{max} = 3$.

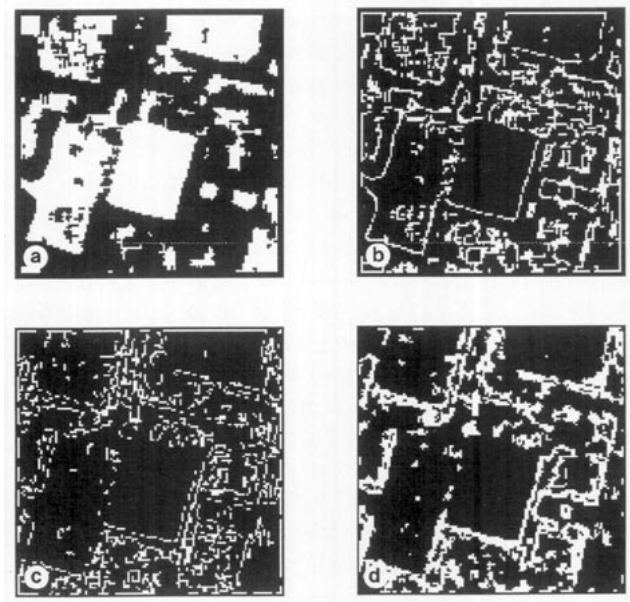

FIG. 7. Selection masks for the result in Fig. 6d. (a) 7 × 7 windows: 39.5%. (b) 5 × 5 windows: 20.4%. (c) 3 × 3 windows: 16.0%. (d) Adaptive least squares: 24.1%.

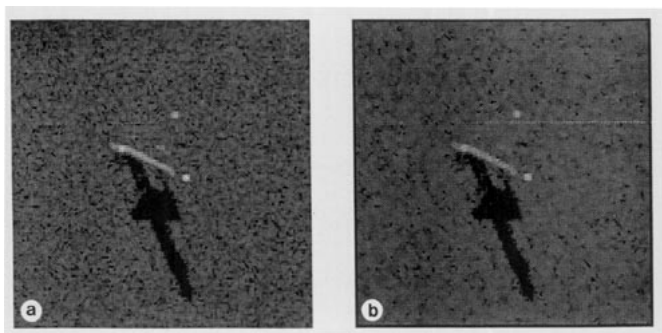

FIG. 8. Multiresolution adaptive smoothing of a SAR image generated by the SARSIM of the Analytic Sciences Corp. (a) Input. (b) Multiresolution adaptive smoothing, $p_{max} = 3$.

technique is simpler and includes additional safeguards by using the robust mode estimator. The long tails of the distributions in Fig. 4 prove the need of robust approaches.

An important property of the MAS algorithm is its hierarchical structure which allows implementation on image pyramids [17]. In this case the image is analyzed at the resolutions corresponding to successive levels of the pyramid: 2×2, 4×4, 8×8. Since the processing is no longer pixel based, the rigid pyramid structure can introduce artifacts. The artifacts are eliminated by combining the results obtained for the input being shifted around. Note that all variances can be computed recursively and the modes can be detected at the apex of the pyramid.

The technique presented in this paper is an example of a more general paradigm. Assume that many nonrobust computational modules, of which about half provide unbiased estimates of an invariant, are available. In our case, these modules are the windows at a given resolution and the invariant is the true value of the stationary noise variance. A simple robust operation can then recover the reliable estimate for the invariant. In the MAS algorithm, the mode detection is that robust operation. Once the close-to-correct value of the invariant is known, the computational modules which provided "good" estimates can be selected. In our case the windows yielding variances smaller than the mode were used. Since only the "good" modules are now taken into account, the final result is robust relative to the assumptions on which the nonrobust computational modules were based. This paradigm is not restricted to image smoothing and can be applied to other computer vision tasks as well.

ACKNOWLEDGMENTS

We would like to thank one of the reviewers whose detailed comments greatly improved the presentation of the paper. Peter Meer and Kyujin Cho acknowledge the support by the National Science Foundation under Grant IRI-9210861, Rae-Hong Park the support of the KOSEF Post-Doctoral Fellowship. Part of this work was done while the first two authors were with the Center for Automation Research, University of Maryland at College Park.

REFERENCES

1. H. H. Arsenault and G. April, Properties of speckle integrated with a finite aperture and logarithmically transformed, *J. Opt. Soc. Am.* **66,** 1976, 1160–1163.
2. T. R. Crimmins, Geometric filter for speckle reduction, *Appl. Opt.* **24,** 1985, 1438–1443.
3. J. Crespo and R. W. Schafer, Image partition using an iterative multiresolution smoothing algorithm, In *Proceedings, IEEE International Conference on Acoustics, Speech, and Signal Processing, San Francisco, March 23–26, 1992.* Vol. III, 561–564.
4. V. S. Frost, J. A. Stiles, K. S. Shanmugan, and J. C. Holtzman, A model for radar images and its application to adaptive digital filtering of multiplicative noise, *IEEE Trans. Pattern Anal. Mach. Intell.* **PAMI-4,** 1982, 157–166.
5. J. W. Goodman, Some fundamental properties of speckle, *J. Opt. Soc. Am.* **66,** 1976, 1145–1150.
6. R. M. Haralick and L. Watson, A facet model for image data, *Comput. Graph. Image Process.* **15,** 1981, 113–129.
7. D. T. Kuan, A. A. Sawchuk, T. C. Strand, and P. Chavel, Adaptive noise smoothing filter for images with signal-dependent noise, *IEEE Trans. Pattern Anal. Mach. Intell.* **PAMI-7,** 1985, 165–177.
8. D. T. Kuan, A. A. Sawchuk, T. C. Strand, and P. Chavel, Adaptive restoration of images with speckle, *IEEE Trans. Acoust. Speech, Signal Process.* **ASSP-35,** 1987, 373–383.
9. J.-S. Lee, Digital image enhancement and noise filtering by use of local statistics, *IEEE Trans. Pattern Anal. Mach. Intell.* **PAMI-2,** 1980, 165–168.
10. J.-S. Lee, Refined filtering of image noise using local statistics, *Comput. Graphics Image Process.* **15,** 1981, 380–389.
11. J. S. Lim and H. Nawab, Techniques for speckle noise removal, *Opt. Eng.* **20,** 1981, 472–480.
12. A. Lopes, R. Touzi, and E. Nezry, Adaptive speckle filters and scene heterogeneity, *IEEE Trans. Geosci. Remote Sensing* **GRS-28,** 1990, 992–1000.
13. B. Mahesh, W.-J. Song, and W. A. Pearlman, Adaptive estimators for filtering noisy images, *Opt. Eng.* **29,** 1990, 488–494.
14. G. F. McLean and M. E. Jernigan, Indicator functions for adaptive image processing, *J. Opt. Soc. Am. A* **8,** 1991, 141–156.
15. D. Mintz, P. Meer, and A. Rosenfeld, Consensus by decomposition: A paradigm for fast high breakdown point robust estimation, in *Proceedings, 1991 DARPA Image Understanding Workshop, La Jolla, CA, January 1992,* pp. 345–362.
16. S. I. Olsen, Estimation of noise in images: An evaluation, *CVGIP: Graphical Models Image Process.* **55,** 1993, 319–323.
17. R.-H. Park and P. Meer, Edge-preserving artifact-free smoothing with image pyramids, *Pattern Recognit. Lett.* **12,** 1991, 467–475.
18. P. Perona and J. Malik, Scale space and edge detection using anisotropic diffusion, *IEEE Trans. Pattern Anal. Mach. Intell.* **PAMI-12,** 1990, 629–639.
19. W. H. Press, B. P. Flannery, S. A. Teukolsky, and W. T. Vetterling, *Numerical Recipes,* Cambridge Univ. Press, Cambridge, 1988.
20. P. J. Rousseeuw and A. M. Leroy, *Robust Regression and Outlier Detection,* Wiley, New York, 1987.
21. F. Safa and G. Flouzat, Speckle removal on radar imagery based on mathematical morphology, *Signal Proc.* **16,** 1989, 319–333.
22. P. Saint-Marc, J. S. Chen, and G. Medioni, Adaptive smoothing: A general tool for early vision, *IEEE Trans. Pattern Anal. Mach. Intell.* **PAMI-13,** 1991, 514–530.
23. M. Tur, K. C. Chin, and J. W. Goodman, When is speckle noise multiplicative? *Appl. Opt.* **21,** 1982, 1157–1159.
24. M. Unser, Improved restoration of noisy images by adaptive least-squares post-filtering, *Signal Process.* **20,** 1990, 3–14.
25. Y. Wu and H. Maître, A speckle suppression method for SAR images using maximum homogeneous region filters, *Opt. Eng.* **31,** 1992, 1785–1792.